Phonon transport at interfaces between different phases of silicon and germanium

Cite as: J. Appl. Phys. **121**, 025102 (2017); https://doi.org/10.1063/1.4973573 Submitted: 16 August 2016 . Accepted: 21 December 2016 . Published Online: 09 January 2017

Kiarash Gordiz, and Asegun Henry







ARTICLES YOU MAY BE INTERESTED IN

Phonon transport at interfaces: Determining the correct modes of vibration Journal of Applied Physics 119, 015101 (2016); https://doi.org/10.1063/1.4939207

Nanoscale thermal transport. II. 2003-2012

Applied Physics Reviews 1, 011305 (2014); https://doi.org/10.1063/1.4832615

Nanoscale thermal transport

Journal of Applied Physics 93, 793 (2003); https://doi.org/10.1063/1.1524305







Phonon transport at interfaces between different phases of silicon and germanium

Kiarash Gordiz¹ and Asegun Henry^{1,2,3,a)}

¹George W. Woodruff School of Mechanical Engineering, Georgia Institute of Technology, Atlanta, Georgia, 30332, USA

²School of Materials Science and Engineering, Georgia Institute of Technology, Atlanta, Georgia 30332, USA ³Heat Lab, Georgia Institute of Technology, Atlanta, Georgia 30332, USA

(Received 16 August 2016; accepted 21 December 2016; published online 9 January 2017)

Current knowledge and understanding of phonon transport at interfaces are wholly based on the phonon gas model (PGM). However, it is difficult to rationalize the usage of the PGM for disordered materials, such as amorphous materials. Thus, there is essentially no intuition regarding interfaces with amorphous materials. Given this gap in understanding, herein we investigated heat conduction at different crystalline and amorphous Si/Ge interfaces using the recently developed interface conductance modal analysis method, which does not rely on the PGM and can therefore treat an interface with a disordered material. The results show that contrary to arguments based on lower mean free paths in amorphous materials, the interface conductances are quite high. The results also show that the interfacial modes of vibration in the frequency region of 12–13 THz are so important that perturbing the natural vibrations with velocity rescaling heat baths (i.e., in non-equilibrium molecular dynamics simulations) affects the conductance even when the heat baths are >60 nm away from the interface. The results suggest that it may be possible to affect interfacial heat transfer by perturbations very far away from the interface, which is an effect that cannot be explained or even rationalized by the traditional paradigm that stems from the Landauer formalism. *Published by AIP Publishing*. [http://dx.doi.org/10.1063/1.4973573]

I. INTRODUCTION

When heat flows through the junction of two solid materials, a discontinuity in the temperature profile at the interface occurs due to the thermal interface resistance (TIR). The magnitude of this temperature jump (ΔT) is proportional to the heat flux through the interface (Q) and the TIR. The inverse of TIR, the thermal interfacial conductance (TIC) is often denoted as G. The relation between the heat flux, temperature jump, and TIC can then be written as $Q = G\Delta T$. Since the first experimental observations of TIR, 1,2 different theoretical models have been proposed to explain the transfer of heat across interfaces and to predict TIC. The acoustic mismatch model (AMM),^{3,4} the diffuse mismatch model (DMM),^{5–7} atomistic Green's function (AGF),^{8,9} wave-packet (WP) analysis,^{10,11} and frequency domain perfectly matched layer (FD-PML) method^{12,13} are notable examples of these models. Although each of these techniques is devised for different sets of operating conditions (e.g., temperature range, interface quality, etc.), they are all based on the phonon gas model (PGM) and usually invoke the Landauer formalism. ^{14–16} In the PGM, phonons are modeled as travelling quasi-particles with energies ($\hbar\omega$) and well-defined velocities, which are determined by the group velocity (v_g) , that are incident on the interface. The Landauer formalism then describes TIC in terms of what fraction of the energy of each incident phonon is transmitted to the other side of the interface. Mathematically, the Landauer formalism for phonon transport at the interface of two solid materials, A and B, is formulated as ^{14,17}

$$G = \sum_{p_A} \left[\frac{1}{V_A} \sum_{k_{x,A} = -k_{max}}^{k_{max}} \sum_{k_{y,A} = -k_{max}}^{k_{max}} \sum_{k_{z,A} = 0}^{k_{max}} v_{z,A} \hbar \omega \tau_{AB} \frac{df(\omega, T)}{dT} \right], \tag{1}$$

where the summations are performed over different polarizations (p) and allowed wave vectors $(k_{x,y,z})$ in material A so that only phonons with velocities incident on the interface are counted, 14 V_A is the volume of side A, $v_{z,A}$ is the phonon group velocity normal to the interface, \hbar is Planck's constant divided by 2π , ω is the frequency of vibration, τ is the transmission probability for the mode of vibration, f is the Bose-Einstein distribution function, and T is temperature. It should be noted that in the Landauer formulation, v_g needs to be calculated for all the modes of vibration in the system and such a calculation is only possible for crystalline solids. Therefore, application of PGM based methods to the interfaces of amorphous materials and alloys is highly questionable, since v_q cannot be defined for most of the vibrational modes, as most of the modes of vibration in amorphous materials are not of propagating nature. ^{18–23} Thus, based on these existing frameworks, there is no obvious insight one can derive from the governing model itself. Instead one can only resort to very approximate physical arguments.

With respect to thermal conductivity (TC), different approaches such as the Allen-Feldman method (A-F)^{18,24} or the virtual crystal approximation (VCA)²⁵ are able to provide some degree of insight into the heat transfer in amorphous

a) Author to whom correspondence should be addressed. Electronic mail: ase@gatech.edu

solids and alloys, respectively. Using these techniques, one can explain the order of magnitude difference between the TC of crystalline and amorphous solids. However, no similar methods exist to predict how TIC varies when one or both sides of an interface are amorphous. The only approximate physical insight one might be able to justify is possibly that an interface with an amorphous material is likely to exhibit low conductance since amorphous material thermal conductivities are typically very low by comparison to crystals. Thus, in essence, the only expectation one might derive about an interface with an amorphous material is that the modes have short "effective mean free paths" and thus they are unlikely to be effective at moving heat across an interface. Furthermore, one might also argue that if the interface is between an amorphous material and a crystal, the modes in the crystal may have a strong likelihood of scattering at the interface, because the mode character is expected to change dramatically at the interface, thus requiring some type of mode conversion/exchange, which would require a scattering event. However, contrary to this approximate intuition, a recent study²⁶ measured a larger TIC at the interface of graphite and amorphous SiC than at the interface of graphite and crystalline SiC. The reason for such a nonintuitive result is currently unknown, but likely due to the action of very different mechanisms than what are normally understood to take place in crystalline materials.

On the one hand, in crystalline materials, phonon transport is described based on purely propagating modes of vibration (i.e., the PGM). On the other hand, in amorphous solids, transport occurs because of interactions between three distinct types of vibrations: propagons, diffusions, and locons, among which only propagons exhibit a propagating nature. 18 None of the more well-established approaches 18,24,25 are able to explain how these different types of vibrations interact to transfer energy across an interface. For example, the mechanism whereby a propagating mode on the crystalline side couples with diffusion on the amorphous side can be postulated but has never been studied in detail. In addition, it is unknown whether the localized modes at the interface can facilitate the transfer of energy at a disproportionally higher rate between the two sides in all situations similar to how they behaved at the interface of crystalline silicon (Si) and germanium

Si/Ge is a prototypical system that has been extensively studied in the literature, largely due to its applications in thermoelectrics.^{29,30} Amongst the extensive literature on thermal transport across Si/Ge interfaces, most studies have been dedicated to the crystalline interfaces. 10,27,28,31-39 To the authors' knowledge, none of the reports that have investigated noncrystalline Si/Ge interfaces have calculated the conductance for an individual interface. In a recent study, Giri et al. examined the effect of crystalline/amorphous Si/Ge interfaces on heat transfer through confined films and superlattices. 40 In their study, the reported resistances are the total resistance for the film (i.e., the summation of resistances at the bulk and at the interfaces). In another study, Giri et al. studied the amorphous Si/Ge superlattices and utilized a thermal circuit model (based on separate calculations for bulk resistances) to calculate the resistance at the interfaces.⁴¹ In this study, however we focus on direct calculation of conductance across

TABLE I. Six distinct interfaces can be formed by joining the c-Si, c-Ge, a-Si, a-Ge structures: c-Si/c-Ge, c-Si/a-Ge, a-Si/c-Ge, a-Si/a-Ge, c-Si/a-Si, and c-Ge/a-Ge. Only the interfaces on one side of the diagonal are unique.

	c-Si	c-Ge	a-Si	a-Ge	
c-Si		*	*	*	
c-Si c-Ge	*		*	*	
a-Si a-Ge	*	*		*	
a-Ge	*	*	*		

individual interfaces, which as will be shown can provide additional insights that could not be captured by investigating the thermal transport properties from other approaches. We also extend our investigations beyond the c-Si/c-Ge interface and examine all the various combinations of crystalline (henceforth denoted by the prefix c-) and amorphous (henceforth denoted by the prefix a-) Si and Ge to evaluate the effects of different phases of solids on interfacial heat transfer. In this regard, six interfaces have been considered: c-Si/c-Ge, c-Si/a-Ge, a-Si/c-Ge, a-Si/a-Ge, c-Si/a-Si, and c-Ge/a-Ge. Table I shows how these combinations are chosen, and Fig. 1 shows an example supercell used for each of these configurations. In this study, the TIC across these interfaces is calculated and compared and to better understand the contributions by different modes of vibration, the interface conductance modal analysis (ICMA) developed by Gordiz and Henry^{19,42} is employed.

Unlike all the prior works on interfacial heat transfer that resolve phonon-level information, 3,5,8,10,27,43 the ICMA method is not based on the PGM; thus it is able to provide a new perspective on thermal transport through interfaces. In fact, the ICMA method is based on an expression for TIC that was derived from the fluctuation-dissipation theorem. 44-46 These expressions for TIC describe the transport in terms of the degree of correlation in the time varying heat flow across the interface, which can be computed from an equilibrium molecular dynamics (EMD) simulation. The major advancement of Gordiz and Henry, however, was the projection of the interfacial heat flux onto the individual modes of the system⁴² and the recognition that one cannot use the modes associated with the bulk materials to properly describe the interfacial heat flow. 19 Moreover, Gordiz and Henry have shown that, based on the degree of localization of vibrational energy near the interface, the modes of vibration can be classified into four independent classes of vibration, namely, $\langle 1 \rangle$ extended modes, $\langle 2 \rangle$ partially extended mode, $\langle 3 \rangle$ isolated mode, and (4) interfacial modes. 19 Extended modes are delocalized over the entire system, and their population scales with larger degrees of density of states (DOS) overlap between the sides of the interface, ⁴⁷ since their vibrations exist on the bulk of both sides of the interface. Partially extended modes have vibrations on one side of the interface; however the vibrations only partially extend through the interface and to the other side. Isolated modes exist only on one side of the interface and do not include participation near the interface. Interfacial modes are localized/peaked near the interface and predominantly incorporate interfacial atoms into their vibrations. Previous investigations of Lennard-Jones solids, ¹⁹

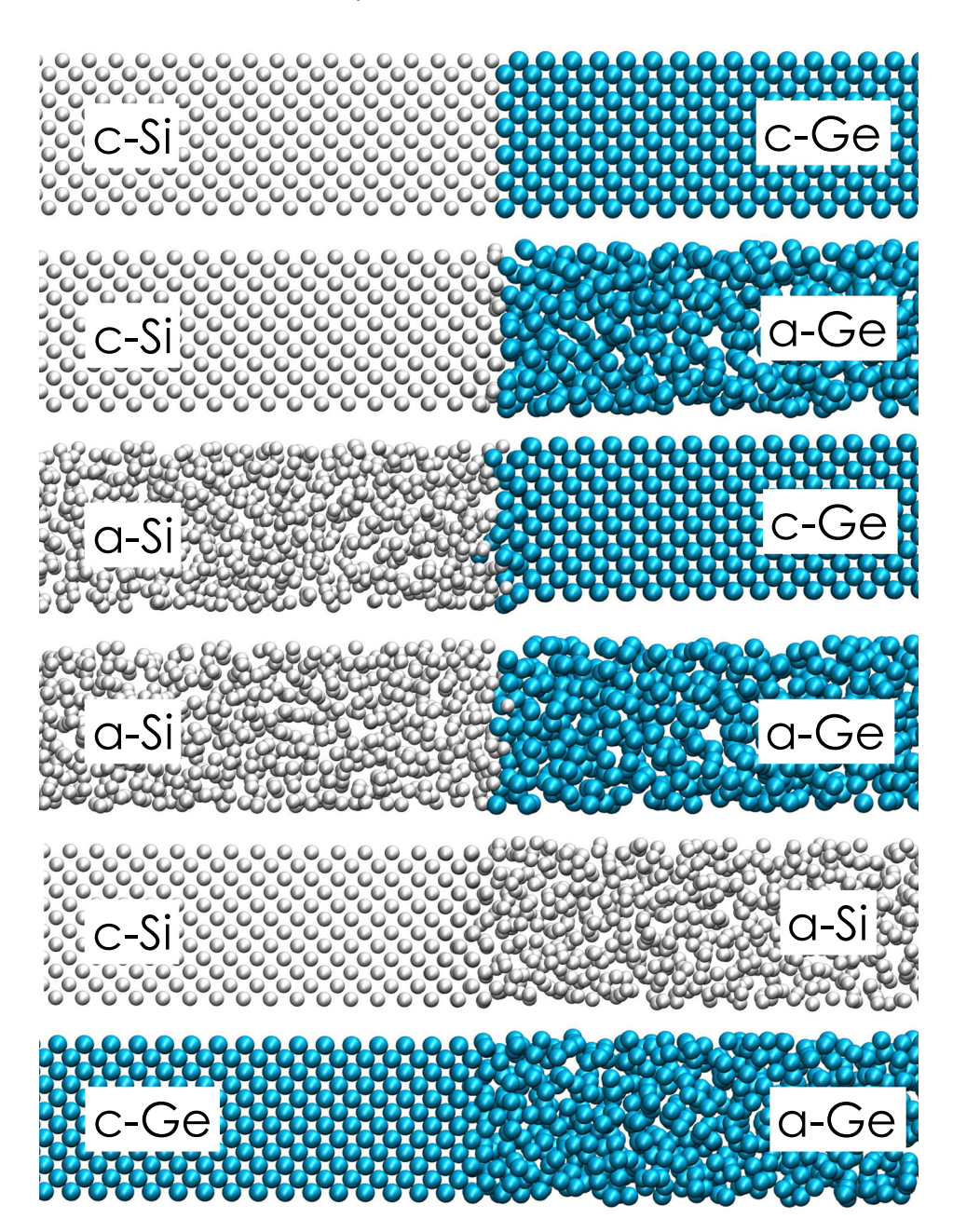


FIG. 1. Schematics of the six formed interfaces between c-Si, a-Si, c-Ge, and a-Ge structures. White and cyan spheres represent Si and Ge atoms, respectively.

c-Si/c-Ge,²⁸ and InP/InGaAs⁴⁷ interfaces have shown that the population of interfacial modes is usually much smaller than the other types of vibrations; however they exhibit the largest contribution to the conductance on a per mode basis. Thus, one of the key benefits of using ICMA is that it can describe any of the modes that exist in an interfacial structure, which can have a variety of different types of mode characters. However, because the PGM based descriptions require that all modes be treated as propagating modes, they are unable to account for the effect that an interface has on the mode character in a given structure. Therefore, in this study, the ICMA method not only quantifies, but also provides a rigorous and unified platform for understanding the various contributions to TIC from different phonons in all of the Si/Ge systems described in Table I and Figure 1.

The remaining sections of the manuscript are outlined as follows. The conducted MD simulations are described in

Section II. Section III includes the results of the EMD and non-equilibrium molecular dynamics (NEMD) based ICMA calculations and the corresponding discussions. Lastly, our conclusions are presented in Section IV.

II. SIMULATION AND METHODOLOGY

Here, the ICMA method is first employed in EMD, but is later used in NEMD as well. ⁴² The Tersoff potential ⁴⁸ is used to describe the interactions between the atoms in the system. In the case that one side of the interface was crystalline, the number of unit cells along x, y, and z directions is 3, 3, and 24, respectively. In previous studies of similar systems, Gordiz and Henry showed that the TIC values are converged with less than 5% standard deviation utilizing this system size ^{19,28,42,47} (see Fig. 7 for further discussions). The interface is a plane perpendicular to the z direction, which is parallel to

the [100] crystallographic direction. To generate the structure for the amorphous side, the number of atoms corresponding to the densities of a-Si (\sim 2.29 g/cm³ (Ref. 49)) and a-Ge $(\sim 5.32 \text{ g/cm}^3 \text{ (Ref. 50)})$ are initially randomly positioned in a simulation box with the same dimensions as the crystalline side. The system is then heated to a temperature above its melting point, after which it is guenched to 0 K over a 50 ns simulation time. The two sides are then brought into contact, and the entire system is annealed at 1000 K for 2 ns. This annealing/sintering process is required to ensure the correct positioning of the atoms around their equilibrium sites.⁵¹ Fig. 2 shows the radial distribution function (RDF) of the generated amorphous structures based on this generation scheme. It can be seen that the calculated RDFs show reasonable agreement with experimental values. Periodic boundary conditions are applied in all 3 spatial directions, and a time step of 0.5 fs is used for all simulations. After first relaxing the structures under isobaric-isothermal conditions (NPT) for 1 ns at zero pressure and then under isochoric-isothermal conditions (NVT) for another 1 ns at T = 300K, we simulate the structures in the microcanonical (NVE) ensemble for 10 ns at which point the modal contributions to the heat flux across the interface are calculated. The heat flux contributions are saved and post processed to calculate the mode-mode heat flux correlation functions. 42 Statistical uncertainty, due to insufficient phase space averaging, has been reduced to less than 5% by considering 10 independent ensembles for each case. 52,53 All MD simulations were conducted using the Large-scale Atomic/Molecular Massively Parallel Simulator (LAMMPS) package⁵⁴ and the eigenmodes for each structure were determined from lattice dynamics calculations using the General Utility Lattice Program (GULP).⁵⁵ It should be noted that zero pressure constraint used in our simulations has also been utilized in other MD studies, 40,41 and it helps to more easily find the finite-temperature relaxed structure and volume. However, because of the lattice-mismatch condition that is common in finite size MD simulations, using such a zero pressure constraint does not ensure zero pressure along all three Cartesian coordinates, but at least can provide the minimum stress structure. In our conducted simulations for the c-Si/c-Ge interface, the average values of stress along the x, y, and z directions were $+7.5 \,\mathrm{Pa}$, $+7.5 \,\mathrm{Pa}$, and $+14.6 \,\mathrm{Pa}$, respectively. For the other structures that incorporated an amorphous structure, the stress values along the x, y, and z coordinates acquired higher values equal to $\sim+100$ Pa, +100Pa, and ~-300 Pa, respectively, and the calculated values were less than 10% different among all these structures. After the relaxation procedure is complete for the MD simulations, the authors confirmed that the final densities of the amorphous structures have less than 2% variation from the initial densities mentioned above.

III. RESULTS AND DISCUSSION

A. EMD Simulations

The TIC values for all the interfaces were calculated using EMD at 300 K and are presented in Table II. It can be seen that, except for the c-Ge/a-Ge interface, all of the obtained TIC values differ by less than 40%. This is interesting for two reasons: (1) the TCs of the materials on either side of the interfaces vary greatly – at 300 K, the TCs of naturally occurring c-Si (150 W/m-K (Refs. 57-59)) and c-Ge (70 W/m-K (Ref. 60)) are two orders of magnitude larger than those of a-Si (1 W/m-K (Ref. 61)) and a-Ge (0.5 W/m-K (Ref. 62)); (2) the density of states (DOS) for different modes of vibration across these interfaces is significantly different from each other (see Fig. 3). Particularly, the degree of localization to one side of the interface (i.e., the total population of partially extended, isolated and interfacial modes) is \sim 70% across c-Si/c-Ge interface, while it is only \sim 25% across c-Si/a-Si interface (see Table III), yet these interfaces have comparable values of conductance. Although the overlap in the vibrational density of states has been successful to explain the TIC in many reported instances, ^{26,40,41,63–66} this is not the first time that overlap in the vibrational density of states has served as a poor descriptor for TIC. In addition to others, 67,68 Gordiz and Henry also observed similar results for Lennard-Jones systems.⁶⁹ Further investigations are needed to determine what parameters can explain the TIC variations with a better consistency and accuracy compared to density of states overlap.

Among the available literature where methods that include anharmonicity are used in calculating the conductance across crystalline/amorphous Si/Ge interfaces,

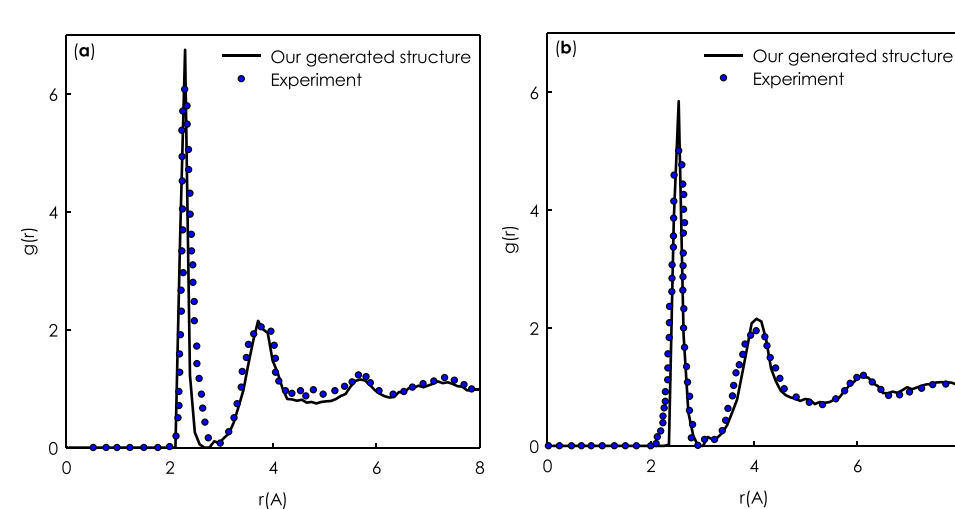


FIG. 2. RDFs for (a) a-Si and (b) a-Ge structures compared to experimental values from Ref. 56.

TABLE II. TIC values for Si/Ge interfaces at $300\,\mathrm{K}~(\mathrm{GWm^{-2}K^{-1}})$ calculated from EMD simulations.

c-Si/c-Ge	0.84
c-Si/a-Ge	0.77
a-Si/c-Ge	0.89
a-Si/a-Ge	1.06
c-Si/a-Si	0.98
c-Ge/a-Ge	0.29

Giri *et al.* have reported the conductance of the a-Si/a-Ge interface to be 1.92 GWm⁻²K⁻¹ (Ref. 41) using NEMD combined with a thermal circuit model to decompose bulk and interfacial resistances, which can explain the difference between their value and our reported EMD values. For the c-Si/c-Ge interface, using NEMD simulations, Giri *et al.*⁴⁰ and Landry and McGaughey⁷⁰ reported the conductance to be 0.36 GWm⁻²K⁻¹ and 0.34 GWm⁻²K⁻¹, respectively, which are in better agreement with our NEMD calculated conductances (see Fig. 9). Additionally, for the c-Si/c-Ge interface, using EMD and Stillinger-Weber interatomic potential,⁷¹ Chalopin *et al.*³² reported a conductance of 0.63 GWm⁻²K⁻¹, the difference of which from our reported value can be attributed to different interatomic-potentials.

The TIC accumulation functions for each of the six configurations were calculated and are shown in Fig. 4. In addition, by using ICMA, the degree of coupling/interaction between each pair of vibrational modes across the interface 19 was calculated and is presented as 2D maps of correlation in Fig. 5. As was pointed out in a recent study by Gordiz and Henry, ²⁸ for the c-Si/c-Ge interface, the modes of vibration in the frequency range of 12-13 THz show a large degree of coupling with all the other modes of vibration in the system (Fig. 5(a)) and contribute almost 15% to the TIC (Fig. 4). The population of these modes in this 12–13 THz region was shown to be less than 0.1% of the total population of modes.²⁸ Additionally, it was shown that while these modes have extended vibrations on the Si side, they also exhibit a large portion of their vibrational energy at the interface²⁸ hence they are considered interfacial modes of vibration¹⁹ (see Fig. 6 for one example of these modes of vibration). By changing the crystallinity of each side of the interface, the highly interacting frequency region of 12–13 THz (Fig. 5(a)) seems to shift to a broader frequency region of vibrations around 10-14 THz for c-Si/a-Ge, a-Si/c-Ge and a-Si/a-Ge interfaces (Figs. 5(b)-5(d)). Although the frequency region of 10-14 THz also contributes largely to the TIC across c-Si/ a-Ge, a-Si/c-Ge and a-Si/a-Ge interfaces (see Fig. 4), all the modes of vibration present within this region contribute on average equally to the TIC. Therefore, unlike the c-Si/c-Ge interface, contributions to interfacial heat transfer across the c-Si/a-Ge, a-Si/c-Ge, and a-Si/a-Ge interfaces are not dominated by a small subset of modes. It is also interesting to note that the highly interacting frequency region of 12–13 THz in the c-Si/c-Ge interface is absent in the c-Si/a-Si and c-Ge/a-Ge interfaces (Figs. 5(e) and 5(f)). In fact, the TIC for these interfaces is largely dependent on the elastic interactions (i.e., auto-correlations) present along the diagonal of the 2D maps of correlation (Figs. 5(e) and 5(f)), which can possibly be attributed to the large population of extended modes in the c-Si/a-Si and c-Ge/a-Ge structures (in which more than 75% of the modes are extended) (see Table III). Extended modes are delocalized; thus they potentially can transfer heat to the other side of the interface without the need to couple to other modes of vibration. 19 Although c-Si/ a-Si and c-Ge/a-Ge interfaces seemingly follow similar mechanisms of interfacial heat transfer (see Figs. 3(e) and 3(f), Table III, and Figs. 5(e) and 5(f)), the conductance across the c-Ge/a-Ge interface is 3.38 times smaller than that of c-Si/a-Si interface. Such a lower conductance for the c-Ge/a-Ge interface can be understood by considering the fact that the absolute values of heat flux across this interface are on average smaller than the ones across the c-Si/a-Si interface. In fact, in our simulations, the average of the absolute values of heat flux at the c-Si/a-Si interface was 2.36 times larger than that of the c-Ge/a-Ge interface. These lower values of interfacial heat flux naturally result in lower values of conductance using both equilibrium and non-equilibrium definition of interface conductance for the c-Ge/a-Ge interface and they arise due to the simple fact that Ge is heavier than Si. Thus, at the same temperature Ge atoms have lower velocities than Si, and since the heat flux itself is directly proportional to the atom velocities on both sides, the low velocities for both a-Ge and c-Ge yield lower overall heat fluxes and conductances.

B. NEMD simulations

As shown in Figs. 3 and 4, the c-Si/c-Ge case is heavily dependent on the interfacial modes present in the 12-13 THz frequency region. Using ICMA formalism, we also know that these interfacial modes have a long tail of vibration on the bulk Si side. Since a substantial portion of their vibration extends through the Si side, we postulated that if one were to perform non-equilibrium MD (NEMD) simulations of this structure, the heat baths might actually perturb these modes. Particularly because the TIC depends so strongly on the presence of these interfacial modes, the unnatural perturbations associated with velocity rescaling in the heat baths can hypothetically affect the TIC across c-Si/c-Ge. Such an effect is interesting because it cannot be described by a scattering based paradigm. In theory, if TIC is truly governed by phonon scattering at the interface, then scattering away from the interface should not affect it.

It should be noted that the Landauer formalism as presented in Eq. (1) is used in many studies for the interface conductance analysis, 3.5.6.9 however such a description follows the equilibrium phonon description, which concludes that there should be no size dependence associated with TIC. However, it should be noted that Landauer theory can be more generally formulated in terms of the non-equilibrium populations that are incident on the interface. 72.73 These non-equilibrium populations will depend on the mean free paths (i.e., the distance a phonon travels from its last phonon-phonon scattering event to the boundary sets its populations). Nonetheless, the majority of the literature still uses the equilibrium formulation of the Landauer theory (Eq. (1)),

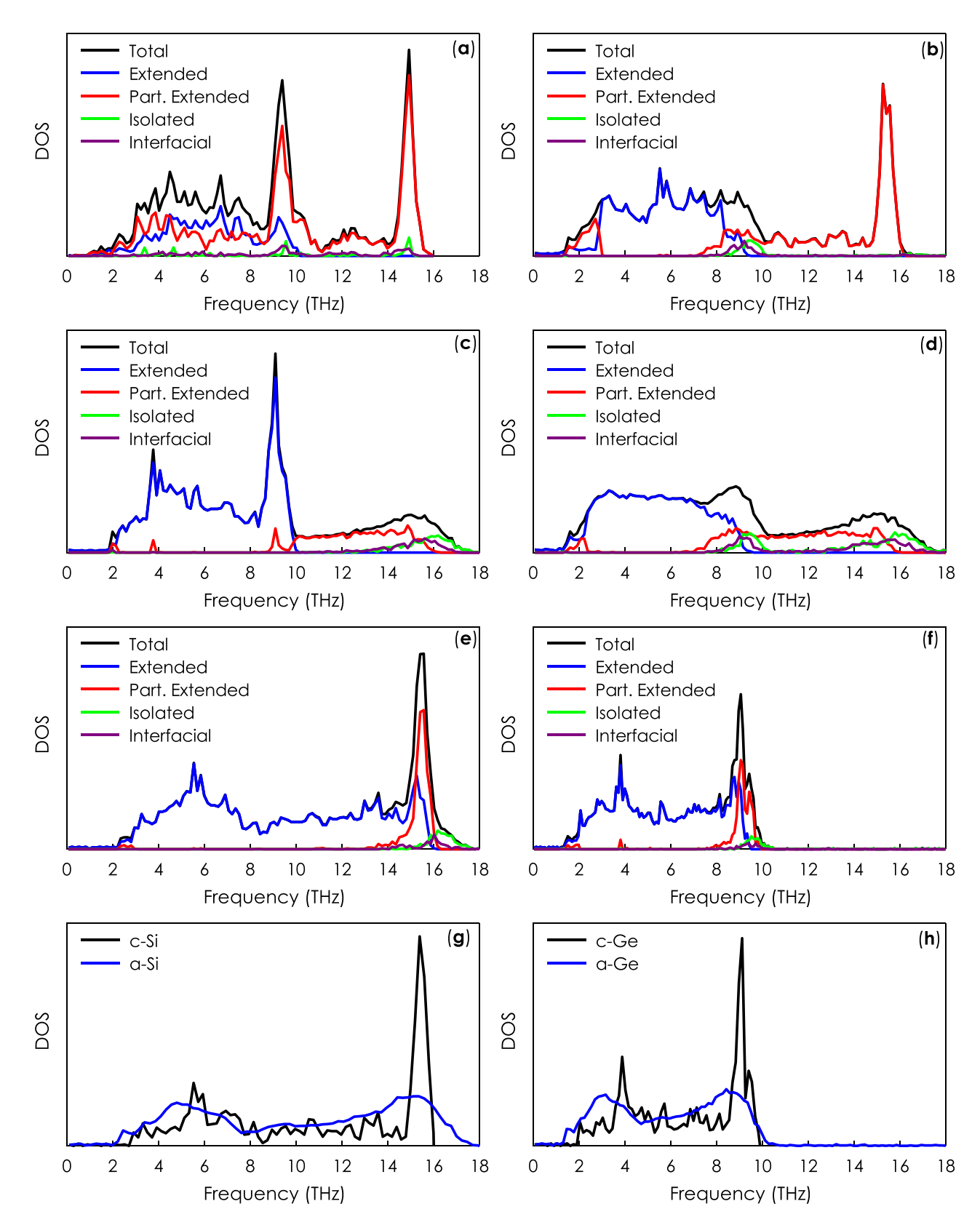


FIG. 3. DOS for the modes of vibration across the (a) c-Si/c-Ge, (b) c-Si/a-Ge, (c) a-Si/c-Ge, (d) a-Si/a-Ge, (e) c-Si/a-Si, and (f) c-Ge/a-Ge interfaces. For comparison, DOS of the bulk crystalline/amorphous Si and crystalline/amorphous Ge structures has also been shown in panels (g) and (h).

whereby no length dependent properties, such as mean free path, enter the description. The only length dependent property is the number of modes in Eq. (1), which are the allowed modes of vibration in the system. ¹⁴ Regarding this issue, Fig. 7 shows that our conducted EMD simulations are effectively

size-independent, which is in agreement with other reports on Si/Ge interfaces. Therefore, it seems that even a small structure with $\sim 3 \times 3 \times 24$ unit cells on each side of the interface includes a sufficient number of modes that TIC varies by less than 5%. (See Fig. 7). Therefore, according to

TABLE III. Number of states for the four different classes of vibration and their contribution to TIC across the c-Si/c-Ge, c-Si/a-Ge, a-Si/a-Ge, c-Si/a-Ge, a-Si/a-Ge, c-Si/a-Si, and c-Ge/a-Ge interfaces. Columns 2–4 describe the fraction of the total number of states (\overline{DOS}) , the percentage contribution to G, and contribution to G divided by a fraction of the total number of states (i.e., contribution to G per mode) $(\overline{G}/\overline{DOS})$, respectively. In agreement with our previous observations, ^{19,28,47} interfacial modes in all of the structures have the highest per mode contribution to the TIC. The TIC value for each interface from Table II is also included for ease of comparison.

Mode type	$\overline{DoS}(\%)$	$ar{G}(\%)$	$ar{G}/\overline{DOS}$	Mode type	$\overline{\textit{DoS}}(\%)$	$ar{G}(\%)$	$ar{G}/\overline{DOS}$
c-Si/c-Ge ($G = 0.84$ GWm $^{-2}$ K $^{-1}$)					c-Si/a-Ge ($G = 0.77$ GWm ⁻² K ⁻¹)		
Extended	29.35	51.99	1.77	Extended	51.27	52.22	1.02
Partially extended	64.24	29.28	0.45	Partially extended	43.11	40.25	0.93
Isolated	3.50	< 0.01	< 0.01	Isolated	3.21	< 0.01	< 0.01
Interfacial	2.90	18.73	6.45	Interfacial	2.39	7.53	3.15
a-Si/c-Ge ($G = 0.89 \text{GWm}^{-2} \text{K}^{-1}$)					a-Si/a-Ge ($G = 1.06$ GWm $^{-2}$ K $^{-1}$)		
Extended	69.16	62.26%	0.90	Extended	56.23	54.71	0.97
Partially extended	19.19	25.72	1.34	Partially extended	24.36	25.99	1.07
Isolated	6.62	< 0.01	< 0.01	Isolated	11.24	< 0.01	< 0.01
Interfacial	5.01	12.02	2.40	Interfacial	8.16	19.30	2.33
c-Si/a-Si ($G = 0.98 \text{GWm}^{-2} \text{K}^{-1}$)					c-Ge/a-Ge ($G = 0.29 \text{GWm}^{-2} \text{K}^{-1}$)		
Extended	77.73	83.61	1.08	Extended	79.93	85.75	1.07
Partially extended	16.20	7.70	0.48	Partially extended	15.30	7.94	0.52
Isolated	4.00	< 0.01	< 0.01	Isolated	3.36	< 0.01	< 0.01
Interfacial	2.05	8.69	4.24	Interfacial	1.38	6.31	4.57

the standard picture, for system sizes beyond $3 \times 3 \times 24$, there should not be any size dependence for the TIC. However, in concept, when one performs velocity rescaling during NEMD simulations, one effectively disrupts mode amplitudes artificially, which can hinder a mode's ability to naturally couple to other modes of vibration and transfer energy. Thus, even though the scattering picture may be useful in many contexts, the existence of an effect on TIC by perturbing modes far away from the interface would serve as evidence to support the notion that the true picture is instead one of correlation/coupling between modes, and not scattering. However, this effect might be reduced for larger and larger structures as the perturbations (e.g., the region of heat input) are moved farther from the interface. Nonetheless, it is also possible that the effect may never completely vanish, since these modes penetrate through the body of the silicon portion (Fig. 6). If true, this would be the first report of such a size effect and would be quite notable, since it would strongly confirm the concept that the interfacial modes exist and can be affected by perturbative stimuli far away from the interface.

To investigate this potential phenomenon, we conducted NEMD simulations using periodic boundary conditions in all Cartesian directions. The cross sections of the structures in the NEMD simulations are of equal dimensions as the supercells used in the EMD simulations. Hot and cold heat baths were placed at midpoints between the (periodic) interfaces (Fig. 8). A thermal power equal to 220 nW is input to the system at the hot bath and removed from the system at the cold bath. The system is simulated for 4 ns to reach steady state, after which the temperature profile (see Fig. 8) remains constant throughout the structure. The temperature profile was then averaged for 2 ns, from which the temperature jump (ΔT_K) at the interface was calculated across the interface. The TIC at the interface can then be calculated from

$$G = \frac{\bar{Q}}{\Delta T_K},\tag{2}$$

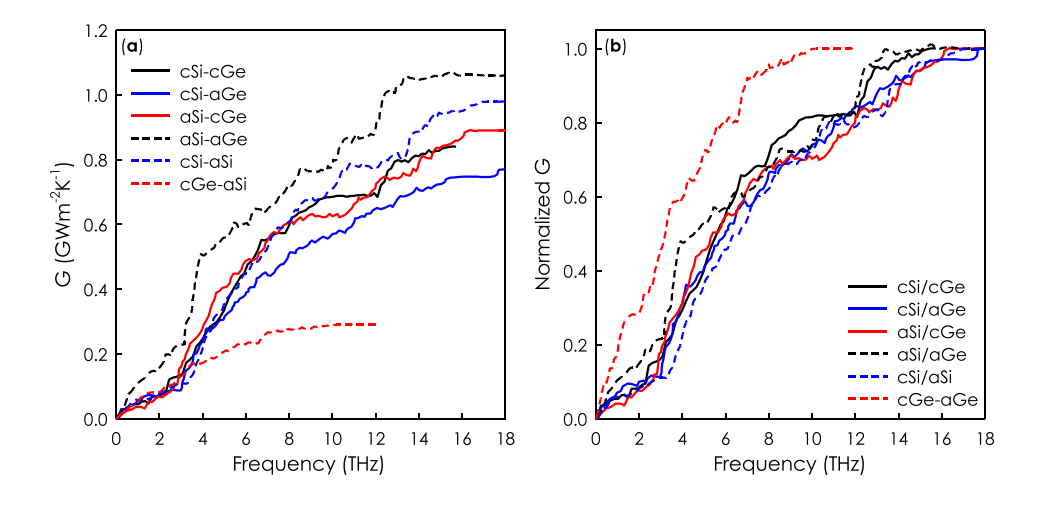


FIG. 4. (a) Non-normalized and (b) normalized TIC accumulation functions for Si/Ge interfaces at T = 300 K.

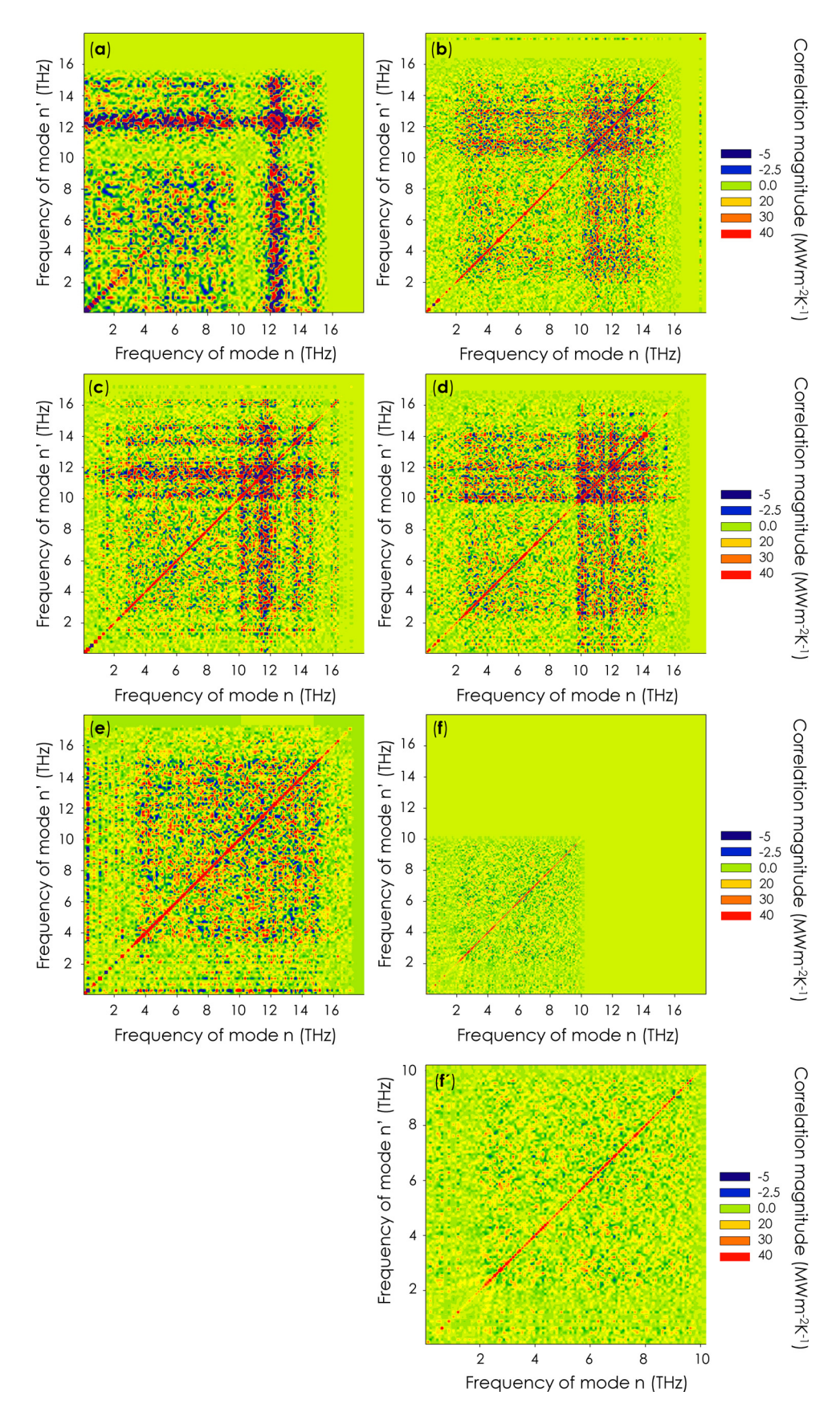


FIG. 5. 2D maps showing the magnitude of correlations/interactions across the (a) c-Si/c-Ge, (b) c-Si/a-Ge, (c) a-Si/c-Ge, (d) a-Si/a-Ge, (e) c-Si/a-Si, and (f) c-Ge/a-Ge interfaces as elevations above the plane of two frequency axes. (f') shows a magnified view for the interactions across the c-Ge/a-Ge interface (panel (f)). The values presented on the maps have units of $MWm^{-2}K^{-1}$.

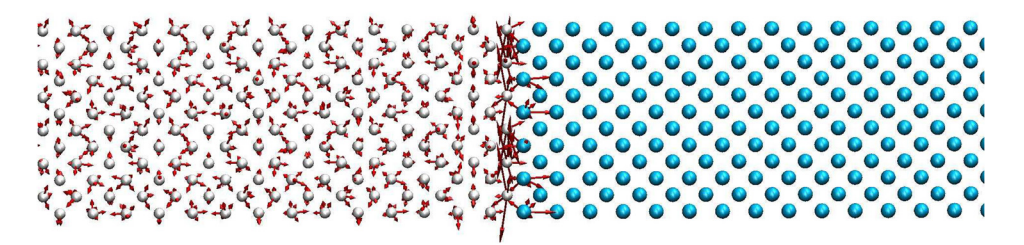
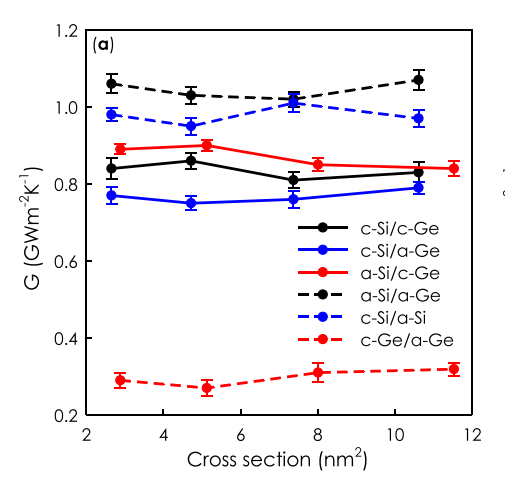


FIG. 6. Eigen vectors for one of the interfacial modes in the 12–13 THz region across the c-Si (white)/c-Ge (cyan) interface.

where \bar{Q} is the time-averaged heat flux through the interface. Five independent ensembles were simulated for improved phase-space averaging. Different values of thermal power lead to different values of temperature jump. However, the authors confirmed that TIC values in the conducted simulations were insensitive to the chosen values of thermal power. In fact, varying the thermal power from 5 nW to 300 nW only changed the calculated TIC values by less than 2%.

The results are presented in Fig. 9 and confirm the hypothesis that size effects can have a significant impact on TIC. All the NEMD calculated TIC values except for the a-Si/a-Ge interface were found to be significantly lower than the values calculated from EMD. Since the EMD values are independent of the system size (see Fig. 7), for a clearer comparison with NEMD values, they are shown normalized to the corresponding EMD value for the same structure. The large difference between the EMD and NEMD values for conductance across the a-Si/a-Ge interface is surprising. One reason for such a discrepancy can be attributed to the fact that due to the low thermal conductivities of amorphous structures no clear temperature drop could be detected across the a-Si/a-Ge interface. This can be the reason this interface appears to have a higher TIC than the equilibrium value, as the uncertainty associated with the calculation is larger. In this regard, as was pointed out in a recent study by Giri et al.40 EMD calculations can provide better predictions for TIC across such interfaces. Further comparisons between EMD and NEMD simulations for TIC analysis can be found in a study by Merabia and Termentzidis.⁷⁴ It may also be possible that the mechanism for transport between diffusions and locons is enhanced by the heat bath perturbation while it is suppressed for propagating modes existing in a crystalline material. Further study would be needed to determine if this is true, but it if so this study would provide some supporting evidence to that effect. In addition, Fig. 9 shows that the NEMD TIC values for the c-Si/c-Ge interface exhibit the largest discrepancy with the EMD values and exhibit the strongest size dependence. Perturbing the vibrations by placing the heat baths at the bulk of the materials, even far from the interface (e.g., >60 nm), can have a noticeable effect on TIC, even for a system with a length >60 nm. This observation cannot be understood through the standard PGM/Landauer formalism, since it would be difficult to rationalize how perturbing a mode far from the interface would affect its transmissivity at the interface. Landry and McGaughey⁷⁰ have shown that by simulating longer structures (e.g., >150 nm) convergence for conductance across c-Si/c-Ge interface using the NEMD approach can be achieved. They also observed convergence between their NEMD calculations and a Landauer-based approach for interface analysis and observed good agreement.

To further confirm that this effect is in fact caused by the aforementioned mechanism, we computed the conductance accumulations using the NEMD implementation of ICMA. 42 The TIC accumulation function from this approach is calculated and presented in Fig. 10, which shows that in the NEMD simulation, the ability of interfacial modes to couple to other modes is hampered by the heat bath. Here it is interesting to see that it is primarily the contributions of other modes that would have coupled to the 12-13 THz interfacial modes that are mostly affected. Thus, the observations indicate that mode-mode correlation/coupling in the bulk of a material may be a core mechanism for interfacial heat transfer, as was also suggested by Wu and Luo.⁷⁵ This is particularly interesting because it suggests a rather different physical picture is needed as compared to the standard PGM/Landauer model. Having observed this effect, to further test our understanding, we constructed an alternative system by separating the heat baths by 2 additional layers of c-Si and c-Ge, effectively simulating three periods of a



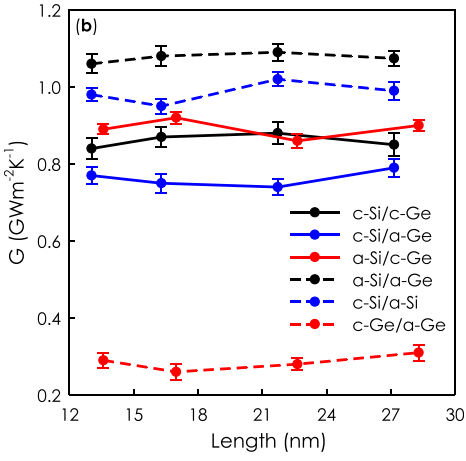


FIG. 7. The effects of increasing the (a) cross section and (b) length of the structure on the TIC of different Si/Ge interfaces from EMD simulations.

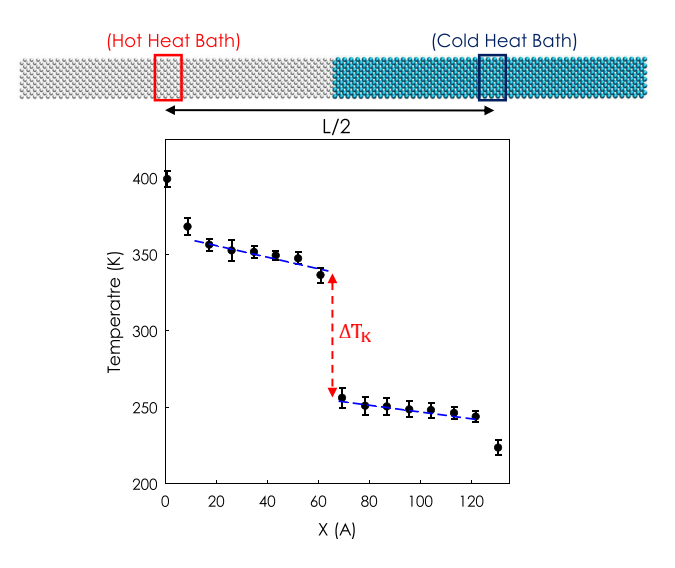


FIG. 8. Schematic of the NEMD implementation to calculate TIC. Hot and cold heat baths are assigned to red and blue blocks, respectively. White and cyan spheres represent Si and Ge atoms, respectively. Temperature distribution is also provided, which clearly shows the temperature drop (Kapitza resistance) around the interface.

superlattice structure (Fig. 11). If our understanding of the effect of the heat baths is correct, then for this larger structure, we would expect a markedly reduced effect from heat baths on the middle interface, which does not contain materials in contact that are directly perturbed by the heat baths. In this way, the heat bath effect should be most pronounced for the two other interfaces, but possibly negligible for the middle interface.

Such a test is again a potentially strong indicator that the scattering based interpretation of interfacial heat flow may be problematic, even in the case of two crystals, where the PGM is most well justified. This is because the three periods of the superlattice structure are identical; thus one would expect by all scattering based arguments that they should all exhibit the

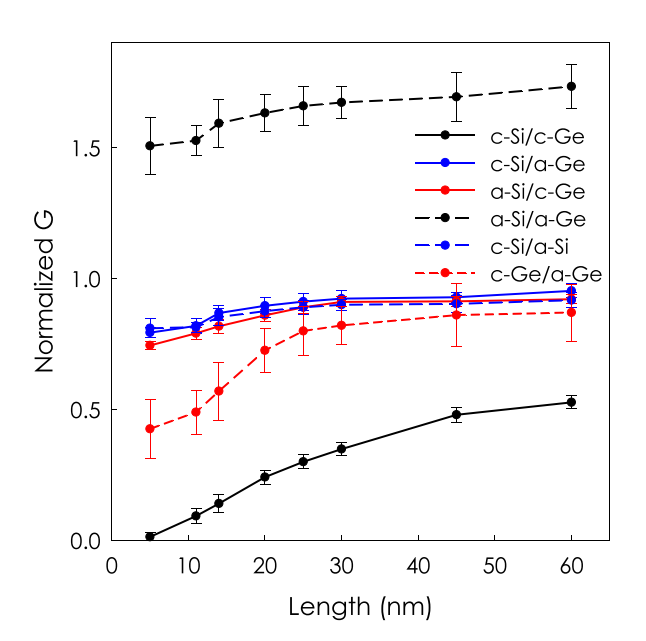


FIG. 9. Normalized TIC values for Si/Ge interfaces obtained from NEMD simulations as a function of the system length. The NEMD values are normalized to the corresponding EMD value for the same structure.

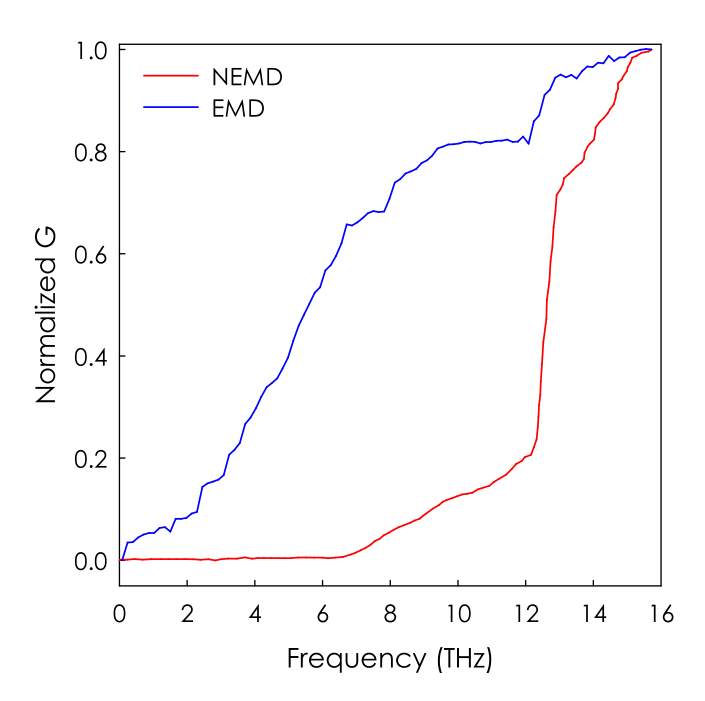


FIG. 10. Modal contributions to TIC for the c-Si/c-Ge interface calculated from the NEMD and EMD implementations of ICMA.

same TIC. This perspective is based on the fact that the most prevalent picture for interfacial transport is based on the PGM/Landauer formalism, which in no way suggests that transmission at an interface should in any way be coupled to or affected by scattering away from the interface. In the current view, the bulk and interface scattering are viewed as essentially independent phenomena, and thus the effect that the heat bath would have 10's of nanometers away from the interface should be negligible, thereby leading to the same TIC for all three superlattice period interfaces.

The results of this test are shown in Fig. 11, which confirms our hypothesis by showing that the unperturbed interface in the middle has a higher TIC, as visibly evidenced by

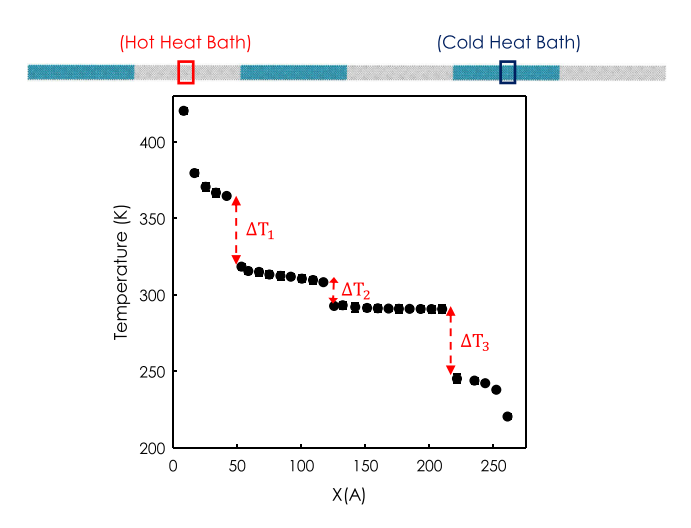


FIG. 11. Schematic of the NEMD implementation across the superlattice structure. Hot and cold heat baths are assigned to red and blue blocks, respectively. White and cyan spheres represent Si and Ge atoms, respectively. Temperature distribution is also provided, which clearly shows that the temperature drop across the interface with unperturbed vibrations (ΔT_2) is smaller than the drop across the interfaces with perturbed vibrations (ΔT_1 and ΔT_3) The TIC across the first and third interfaces is equal to each other and equal to 0.19 GWm $^{-2}$ K $^{-1}$ and across the second interface is 0.64 GWm $^{-2}$ K $^{-1}$.

the noticeably larger temperature drop at the other interfaces (Fig. 11). This result is quite remarkable because the NEMD version of the ICMA formalism does not even involve the calculation of correlation functions. Instead, it is proportional to each mode's average heat flux, and thus it is quite interesting to see that the average mode heat flux itself is actually affected by the heat baths. This then strongly suggests that a coupling/ correlation based perspective is actually in more correct alignment with the actual transport that happens at interfaces, rather than a scattering based perspective. Furthermore, this result also suggests that one may be able to affect transport at a faraway interface, by modifying or perturbing modes artificially in another part of the system. To our knowledge, this is the first report of such an observation, and it can provide a new pathway to dynamic control or influence over TIC, by indirect means in certain material systems, which is quite non-intuitive based on the prevalent PGM paradigm.

IV. CONCLUSION

In conclusion, heat transfer across six different Si/Ge interfaces was investigated using the ICMA method. The interfaces were formed by changing the crystallinity of materials at the sides of the interface. It was shown that although amorphous solids have much lower thermal conductivities, the interface formed at the contact of an amorphous solid does not necessarily exhibit a lower TIC than the crystalline counterpart. Furthermore, it was shown that contrary to the existing intuition, the calculated values of conductance across the investigated interfaces did not follow the trend for the DOS overlap, which is in disagreement with the existing paradigm based on the PGM. Moreover, it was shown that the dominant contribution from interfacial modes at the c-Si/c-Ge interface is not a dominant contribution across the c-Si/a-Ge, a-Si/c-Ge, and a-Si/a-Ge interfaces and such a contribution is lost across the c-Si/a-Si and c-Ge/a-Ge interfaces. In fact, the elastic interactions across the c-Si/a-Si and c-Ge/a-Ge interfaces turned out to be the dominant transport channel for heat transfer across these interfaces, which can be explained by the large population of extended modes across these structures. Additionally, it was shown that the heat transfer across the c-Si/c-Ge interface is so dependent on the interfacial modes in the 12–13 THz frequency region that perturbing these modes (i.e., by NEMD simulations) drastically decreased the contribution from other modes that couple to them and hence the decreased the NEMD-TIC values as compared to EMD. Interestingly, even after lowering the effect of NEMD simulations by placing the heat baths farther from the interface, this effect did not disappear. However, repeating the structure to create an interface that is not directly affected by the heat baths caused the effect to disappear. Such observations are impossible to rationalize using the existing paradigm of PGM and demonstrate that methods such as ICMA, which go beyond the concept of interfacial scattering, are required to explain TIC. The observations suggest that there may be new mechanisms that can be used to control/modulate the heat flow through interfaces (i.e., by perturbing atoms far away from the interface itself).

- ¹P. Kapitza, "The study of heat transfer in helium II," J. Phys. (USSR) **4**, 181–210 (1941).
- ²D. A. Neeper and J. Dillinger, "Thermal resistance at indium-sapphire boundaries between 1.1 and 2.1 K," Phys. Rev. **135**, A1028 (1964).
- ³I. M. Khalatnikov, "Teploobmen mezhdu tverdym telom i geliem-ii," Zh. Eksp. Teor. Fiz. **22**, 687–704 (1952).
- ⁴W. Little, "The transport of heat between dissimilar solids at low temperatures," Can. J. Phys. **37**, 334–349 (1959).
- ⁵E. Swartz and R. Pohl, "Thermal resistance at interfaces," Appl. Phys. Lett. **51**, 2200–2202 (1987).
- ⁶P. E. Hopkins and P. M. Norris, "Effects of joint vibrational states on thermal boundary conductance," Nanosc. Microsc. Therm. 11, 247–257 (2007)
- ⁷C. A. Polanco *et al.*, "Role of crystal structure and junction morphology on interface thermal conductance," Phys. Rev. B **92**, 144302 (2015).
- ⁸N. Mingo and L. Yang, "Phonon transport in nanowires coated with an amorphous material: An atomistic Green's function approach," Phys. Rev. B 68, 245406 (2003).
- ⁹W. Zhang, T. Fisher, and N. Mingo, "The atomistic Green's function method: An efficient simulation approach for nanoscale phonon transport," Numer. Heat TR B-Fund. 51, 333–349 (2007).
- ¹⁰P. K. Schelling, S. R. Phillpot, and P. Keblinski, "Phonon wave-packet dynamics at semiconductor interfaces by molecular-dynamics simulation," Appl. Phys. Lett. 80, 2484–2486 (2002).
- ¹¹C. H. Baker, D. A. Jordan, and P. M. Norris, "Application of the wavelet transform to nanoscale thermal transport," Phys. Rev. B 86, 104306 (2012).
- ¹²R. R. Kakodkar and J. P. Feser, "A framework for solving atomistic phonon-structure scattering problems in the frequency domain using perfectly matched layer boundaries," J. Appl. Phys. 118, 094301 (2015).
- ¹³R. R. Kakodkar and J. P. Feser, "Probing the validity of the diffuse mismatch model for phonons using atomistic simulations," preprint arXiv:1607.08572 (2016).
- ¹⁴G. Chen, Nanoscale Energy Transport and Conversion: A Parallel Treatment of Electrons, Molecules, Phonons, and Photons (Oxford University Press, USA, 2005).
- ¹⁵Z. M. Zhang, *Nano/Microscale Heat Transfer* (McGraw-Hill New York, 2007).
- ¹⁶R. Landauer, "Spatial variation of currents and fields due to localized scatterers in metallic conduction," IBM J. Res. Dev. 1, 223–231 (1957).
- ¹⁷P. E. Hopkins, P. M. Norris, and J. C. Duda, "Anharmonic phonon interactions at interfaces and contributions to thermal boundary conductance," J. Heat Transfer 133, 062401 (2011).
- ¹⁸P. B. Allen, J. L. Feldman, J. Fabian, and F. Wooten, "Diffusons, locons and propagons: Character of atomie yibrations in amorphous Si," Philos. Mag. B 79, 1715–1731 (1999).
- ¹⁹K. Gordiz and A. Henry, "Phonon transport at interfaces: Determining the correct modes of vibration," J. Appl. Phys. 119, 015101 (2016).
- ²⁰T. Gibbons, M. Bebek, C. Stanley, and S. Estreicher, "Phonon-phonon interactions: First principles theory," J. Appl. Phys. 118, 085103 (2015).
- ²¹S. Estreicher, T. Gibbons, and M. Bebek, "Phonons and defects in semi-conductors and nanostructures: Phonon trapping, phonon scattering, and heat flow at heterojunctions," J. Appl. Phys. 115, 012012 (2014).
- ²²S. Estreicher, T. Gibbons, and M. Bebek, "Thermal phonons and defects in semiconductors: The physical reason why defects reduce heat flow, and how to control it," J. Appl. Phys. 117, 112801 (2015).
- ²³S. K. Estreicher, T. M. Gibbons, M. B. Bebek, and A. L. Cardona, in *Solid State Phenomena* (Trans Tech Publications, 2016), pp. 335–343.
- ²⁴P. B. Allen and J. L. Feldman, "Thermal conductivity of disordered harmonic solids," Phys. Rev. B 48, 12581 (1993).
- ²⁵J. M. Larkin and A. J. McGaughey, "Predicting alloy vibrational mode properties using lattice dynamics calculations, molecular dynamics simulations, and the virtual crystal approximation," J. Appl. Phys. 114, 023507 (2013).
- ²⁶M. Li, J. Zhang, X. Hu, and Y. Yue, "Thermal transport across graphene/ SiC interface: Effects of atomic bond and crystallinity of substrate," Appl. Phys. A 119, 415 (2015).
- ²⁷Y. Chalopin and S. Volz, "A microscopic formulation of the phonon transmission at the nanoscale," Appl. Phys. Lett. **103**, 051602 (2013).
- ²⁸K. Gordiz and A. Henry, "Phonon transport at crystalline Si/Ge interfaces: The role of interfacial modes of vibration," Sci. Rep. 6, 23139 (2016).
- ²⁹S. Cecchi *et al.*, "Ge/SiGe superlattices for thermoelectric devices grown by low-energy plasma-enhanced chemical vapor deposition," J. Electron. Mater. **42**, 2030–2034 (2013).

- 30 X. Wang et al., "Enhanced thermoelectric figure of merit in nanostructured n-type silicon germanium bulk alloy," Appl. Phys. Lett. 93, 193121–193123
- ³¹E. Landry and A. McGaughey, "Effect of interfacial species mixing on phonon transport in semiconductor superlattices," Phys. Rev. B 79, 075316 (2009).
- ³²Y. Chalopin, K. Esfarjani, A. Henry, S. Volz, and G. Chen, "Thermal interface conductance in Si/Ge superlattices by equilibrium molecular dynamics," Phys. Rev. B 85, 195302 (2012).
- ³³S. C. Huberman, J. M. Larkin, A. J. McGaughey, and C. H. Amon, "Disruption of superlattice phonons by interfacial mixing," Phys. Rev. B 88, 155311 (2013).
- ³⁴L. Sun and J. Y. Murthy, "Molecular dynamics simulation of phonon scattering at silicon/germanium interfaces," J. Heat Transfer 132, 102403
- ³⁵W. Zhang, N. Mingo, and T. Fisher, "Simulation of interfacial phonon transport in Si-Ge heterostructures using an atomistic Green's function method," J. Heat Transfer 129, 483-491 (2007).
- ³⁶X. Li and R. Yang, "Effect of lattice mismatch on phonon transmission and interface thermal conductance across dissimilar material interfaces," Phys. Rev. B 86, 054305 (2012).
- ³⁷Z. Tian, K. Esfarjani, and G. Chen, "Enhancing phonon transmission across a Si/Ge interface by atomic roughness: First-principles study with the Green's function method," Phys. Rev. B 86, 235304 (2012).
- ³⁸T. Murakami, T. Hori, T. Shiga, and J. Shiomi, "Probing and tuning inelastic phonon conductance across finite-thickness interface," Appl. Phys. Express 7, 121801 (2014).
- ³⁹K. Gordiz and A. Henry, in MRS Proceedings (Cambridge University Press, 2015), pp. 21-26.
- ⁴⁰A. Giri, J. L. Braun, and P. E. Hopkins, "Effect of crystalline/amorphous interfaces on thermal transport across confined thin films and superlattices," J. Appl. Phys. 119, 235305 (2016).
- ⁴¹A. Giri, P. E. Hopkins, J. G. Wessel, and J. C. Duda, "Kapitza resistance and the thermal conductivity of amorphous superlattices," J. Appl. Phys. 118, 165303 (2015).
- ⁴²K. Gordiz and A. Henry, "A formalism for calculating the modal contributions to thermal interface conductance," New J. Phys. 17, 103002 (2015).
- ⁴³K. Sääskilahti, J. Oksanen, J. Tulkki, and S. Volz, "Role of anharmonic phonon scattering in the spectrally decomposed thermal conductance at planar interfaces," Phys. Rev. B 90, 134312 (2014).
- ⁴⁴R. Kubo, "The fluctuation-dissipation theorem," Rep. Prog. Phys. **29**, 255 (1966).
- ⁴⁵J.-L. Barrat and F. Chiaruttini, "Kapitza resistance at the liquid-solid interface," Mol. Phys. 101, 1605-1610 (2003).
- ⁴⁶G. Domingues, S. Volz, K. Joulain, and J.-J. Greffet, "Heat transfer between two nanoparticles through near field interaction," Phys. Rev. Lett. 94, 085901 (2005).
- ⁴⁷K. Gordiz and A. Henry, "Interface conductance modal analysis of lattice matched InGaAs/InP," Appl. Phys. Lett. 108, 181606 (2016).
- ⁴⁸J. Tersoff, "Modeling solid-state chemistry: Interatomic potentials for multicomponent systems," Phys. Rev. B 39, 5566 (1989).
- ⁴⁹J. Custer *et al.*, "Density of amorphous Si," Appl. Phys. Lett. **64**, 437–439 (1994).
- ⁵⁰T. Light, "Density of "amorphous" Ge," Phys. Rev. Lett. **22**, 999 (1969).
- ⁵¹B. Deng, A. Chernatynskiy, M. Khafizov, D. H. Hurley, and S. R. Phillpot, "Kapitza resistance of Si/SiO2 interface," J. Appl. Phys. 115, 084910 (2014).
- ⁵²K. Gordiz, D. J. Singh, and A. Henry, "Ensemble averaging vs. time averaging in molecular dynamics simulations of thermal conductivity," J. Appl. Phys. 117, 045104 (2015).

- ⁵³R. E. Jones and K. K. Mandadapu, "Adaptive Green-Kubo estimates of transport coefficients from molecular dynamics based on robust error analysis," J. Chem. Phys. 136, 154102 (2012).
- ⁵⁴S. Plimpton, "Fast parallel algorithms for short-range molecular dynamics," J. Comput. Phys. 117, 1-19 (1995).
- ⁵⁵J. D. Gale, "GULP: A computer program for the symmetry-adapted simulation of solids," J. Chem. Soc., Faraday Trans. 93, 629-637 (1997).
- ⁵⁶F. Alvarez, C. Díaz, A. A. Valladares, and R. Valladares, "Radial distribution functions of ab initio generated amorphous covalent networks," Phys. Rev. B 65, 113108 (2002).
- ⁵⁷T. Ruf et al., "Thermal conductivity of isotopically enriched silicon," Solid State Commun. 115, 243-247 (2000).
- ⁵⁸A. Inyushkin, A. Taldenkov, A. Gibin, A. Gusev, and H. J. Pohl, "On the isotope effect in thermal conductivity of silicon," Physica Status Solidi C 1, 2995-2998 (2004).
- ⁵⁹R. Kremer *et al.*, "Thermal conductivity of isotopically enriched 28 Si: Revisited," Solid State Commun. 131, 499-503 (2004).
- ⁶⁰V. Ozhogin et al., "Isotope effect in the thermal conductivity of germanium single crystals," JETP Lett. 63, 490-494 (1996).
- ⁶¹D. G. Cahill, H. E. Fischer, T. Klitsner, E. Swartz, and R. Pohl, "Thermal conductivity of thin films: Measurements and understanding," J. Vac. Sci. Technol. A 7, 1259-1266 (1989).
- $^{62}\mbox{D.}$ G. Cahill, S. K. Watson, and R. O. Pohl, "Lower limit to the thermal conductivity of disordered crystals," Phys. Rev. B 46, 6131 (1992).
- ⁶³K. Gordiz, S. V. Allaei, and F. Kowsary, "Thermal rectification in multiwalled carbon nanotubes: A molecular dynamics study," Appl. Phys. Lett. 99, 251901 (2011).
- ⁶⁴S. Shin, M. Kaviany, T. Desai, and R. Bonner, "Roles of atomic restructuring in interfacial phonon transport," Phys. Rev. B 82, 081302 (2010).
- ⁶⁵J. C. Duda et al., "Implications of cross-species interactions on the temperature dependence of Kapitza conductance," Phys. Rev. B 84, 193301
- ⁶⁶T. S. English et al., "Enhancing and tuning phonon transport at vibrationally mismatched solid-solid interfaces," Phys. Rev. B 85, 035438 (2012).
- ⁶⁷A. Rajabpour, S. V. Allaei, and F. Kowsary, "Interface thermal resistance and thermal rectification in hybrid graphene-graphane nanoribbons: A nonequilibrium molecular dynamics study," Appl. Phys. Lett. 99, 051917 (2011).
- ⁶⁸K. Gordiz and S. M. V. Allaei, "Thermal rectification in pristinehydrogenated carbon nanotube junction: A molecular dynamics study," J. Appl. Phys. 115, 163512 (2014).
- ⁶⁹K. Gordiz and A. Henry, "Examining the effects of stiffness and mass difference on the thermal interface conductance between Lennard-Jones solids," Sci. Rep. 5, 18361 (2015).
- ⁷⁰E. Landry and A. McGaughey, "Thermal boundary resistance predictions from molecular dynamics simulations and theoretical calculations," Phys. Rev. B 80, 165304 (2009).
- $^{71}\mathrm{F.~H.}$ Stillinger and T. A. Weber, "Computer simulation of local order in condensed phases of silicon," Phys. Rev. B 31, 5262 (1985).
- ⁷²G. Chen, "Diffusion-transmission interface condition for electron and phonon transport," Appl. Phys. Lett. 82, 991–993 (2003).
- ⁷³S. Simons, "On the thermal contact resistance between insulators," J. Phys. C: Solid State Phys. 7, 4048 (1974).
- ⁷⁴S. Merabia and K. Termentzidis, "Thermal conductance at the interface between crystals using equilibrium and nonequilibrium molecular dynamics," Phys. Rev. B 86, 094303 (2012).
- 75X. Wu and T. Luo, "The importance of anharmonicity in thermal transport across solid-solid interfaces," J. Appl. Phys. 115, 014901 (2014).